JOURNAL OF AGRICULTURAL AND FOOD CHEMISTRY

Food and Beverage Chemistry/Biochemistry

Changes in Nanoscale Chain Assembly in Sweet Potato Starch Lamellae by Downregulation of Biosynthesis Enzymes

Binjia Zhang, Wenzhi Zhou, Dongling Qiao, Zhang Peng, Si-ming Zhao, Liang Zhang, and Fengwei Xie

J. Agric. Food Chem., **Just Accepted Manuscript** • DOI: 10.1021/acs.jafc.8b06523 • Publication Date (Web): 29 Mar 2019

ACS Publications

is published by the American Chemical Society. 1155 Sixteenth Street N.W., Washington, DC 20036

Changes in Nanoscale Chain Assembly in Sweet Potato Starch Lamellae by Downregulation of Biosynthesis Enzymes

Binjia Zhang [a], *Wenzhi Zhou* [b], *Dongling Qiao* [c], *Peng Zhang* [*,b], *Siming Zhao* [a], *Liang Zhang* [d], *Fengwei Xie* [†,e,f]

[a] *Group for Cereals and Oils Processing, Key Laboratory of Environment Correlative Dietology (Ministry of Education), College of Food Science and Technology, Huazhong Agricultural University, Wuhan 430070, China*

[b] *National Key Laboratory of Plant Molecular Genetics, CAS Center for Excellence in Molecular Plant Sciences, Institute of Plant Physiology and Ecology, Shanghai Institutes for Biological Sciences, Chinese Academy of Sciences, Shanghai 200032, China*

[c] *Glyn O. Phillips Hydrocolloid Research Centre at HBUT, Hubei University of Technology, Wuhan 430068, China*

[d] *School of Food Science and Engineering, Yangzhou University, Yangzhou 225127, China*

[e] *Institute of Advanced Study, University of Warwick, Coventry CV4 7HS, United Kingdom*

[f] *International Institute for Nanocomposites Manufacturing (IINM), WMG, University of Warwick, Coventry CV4 7AL, United Kingdom*

KEYWORDS: *Starch; Semicrystalline lamellae; Molecular chain features; X-ray scattering*

ABSTRACT: Granule-bound starch synthase I (GBSSI) and starch branching enzyme I and II (SBEI and SBEII) are crucial enzymes biosynthesizing starches with varied apparent amylose

content and amylopectin branching structure. With a sweet potato (*Ipomoea batatas* [L.] Lam.) Cv. Xushu22, this work shows that downregulating GBSSI (for waxy starch) or SBE (for high-amylose starch) activity allowed the formation of new semicrystalline lamellae (named Type II) in sweet potato starch in addition to the widely reported Type I lamellae. Small-angle X-ray scattering (SAXS) results show that, compared to Type I lamellae, Type II lamellae displayed increased average thickness and thickness distribution width, with thickened amorphous and crystalline components. The size-exclusion chromatography (SEC) data revealed mainly two enzyme-sets (i and ii) synthesizing amylopectin chains. Reducing the GBSSI or SBE activity increased the amounts of amylopectin long chains (degree of polymerization (*DP*) $\geq$ 33). Combined SAXS and SEC analyses indicate that part of these long chains from enzyme-set (i) could be confined to Type II lamellae, followed by *DP* $\leq$ 32 short chains in Type I lamellae and the rest long chains from enzyme-sets (i) and (ii) spanning more than a single lamella.

Introduction

In green plants, the biosynthesis of natural polymers, such as starch, protein and cellulose, stands at the core of providing agro-resources for food and non-food products with demanded features. Starch, a storage carbohydrate in plants (*e.g.*, maize, wheat, rice, potato, cassava, sweet potato), normally serves as a crucial food ingredient offering energy for humans. The biosynthesis of starch is mainly governed by four categories of enzymes, namely, ADP-glucose pyrophosphorylase (AGPase), starch synthases (SSs), starch branching enzymes (SBEs) and starch debranching enzymes (DBEs).[1-2] Modulating the activities of starch biosynthetic enzymes could be a cost-effective approach for the production of starch resources with tailored structure and properties.

Two major starch polymers are biosynthesized during plant growth, namely, relatively linear amylose and highly branched amylopectin.[3] The molecular chains of amylose and amylopectin can assemble on different length scales to form a multilevel structural system of the starch granule, including the whole granule, growth rings, blocklets, semicrystalline lamellae, crystalline structure, and double/single helices.[3-6] The multi-level structural features are closely related to starch properties. To date, maize, rice, and sweet potato starches with varied apparent amylose content (0% to > 50%) and amylopectin branching structure have been produced through modifying the activities of biosynthetic enzymes such as granule-bound starch synthase (GBSS), and/or SBE.[7-8] Compared to the wild-type (WT) starch and the waxy starch with GBSS downregulation, the high-amylose starches (apparent amylose content > 50%) with SBE downregulation show an enhanced granule surface density but a reduced crystallinity degree with B-type crystallites and eventually unique properties such as reduced enzyme susceptibility,[9-10] higher gelatinization temperature,[11] and altered rheological features.[12] Consequently, the high-amylose starches have versatile potentials for functional foods with low glycemic indexes and for

high-performance materials with fascinating functions (*e.g.*, bioactive compound delivery). However, though the main assembly of starch chains on the nanoscale is the semicrystalline lamellar structure, it is still not fully understood how the amylose-content-related biosynthetic enzymes (*e.g.*, GBSS and SBE) tailor the features of starch lamellae, which subsequently determine the starch properties and functionality.

The starch lamellae can be characterized using small-angle X-ray scattering (SAXS) technique with the paracrystalline model,[13-14] the liquid-crystalline model[15] and the linear correlation function.[16] A series of lamellar parameters such as the average thickness of semicrystalline lamellae can be obtained for starches from various origins, *e.g.*, wheat, maize, rice, potato, cassava, and water chestnut.[17-21] It is noteworthy that the change in apparent amylose content probably alters starch lamellar features.[9, 19] For instance, compared to regular starch, high-amylose starches from potato display different lamellar packing whose features can be evaluated using the scattering data and the paracrystalline model with a stacking disorder nature.[19] Nonetheless, to model the structural parameters, this study still needs complicated predefined assumptions for the lamellar structure and the usage of fixed values for partial parameters. Thus, it remains challenging to simply and straightforwardly calculate the lamellar parameters of starches with varied apparent amylose content and amylopectin branching structure from the SAXS data. In addition, starch chains can assemble into crystalline lamellae to construct semicrystalline growth rings. Consistently, the chain length distributions (CLDs) are capable of affecting the lamellar parameters of rice starches with apparent amylose content up to 24%.[22-23] However, the previous studies did not concern how the biosynthetic enzymes (*e.g.*, GBSS and SBE) alter the CLDs of starch and thus its nanoscale chain assembly in lamellae, with apparent amylose content in much wider ranges such as from 0% to >50%.

To this end, a WT sweet potato (*Ipomoea batatas* [L.] Lam.) and its waxy (produced by granule-bound starch synthase I (GBSSI) with downregulated activity) and high-amylose (produced by SBE with downregulated activity) lines were used as the model plants for the biosynthesis of WT and tailored starches with *ca.* 6% to 65% apparent amylose content. The small angle X-ray scattering (SAXS) technique was applied to characterize the semicrystalline lamellae of the starches. Interestingly, a new type of semicrystalline lamellae was found and a fitting method was proposed to resolve the lamellar peak and its subpeaks from the whole SAXS pattern. The fitted lamellar peaks were used to straightforwardly calculate the fine parameters for the two types of starch lamellae with a linear correlation function. Along with that, the CLDs of starch and the related starch biosynthetic enzyme activities were analyzed using the SEC data. Then, from a CLD point of view, we discussed how the GBSSI or SBE downregulation tailors the starch lamellar structure.

Experimental Section

Materials. The sweet potato (*Ipomoea batatas* [L.] Lam.) Cv. Xushu22, a widely used cultivar for starch production in China, was used as the donor cultivar (WT) for modification. A method described previously[24] was applied to generate modified sweet potato plants. One waxy line (namely Waxy-91) with downregulated GBSSI expression and three high-amylose lines (HAM-75, HAM-214, and HAM-234) with downregulated SBE expression were chosen for this study. The expressions of SBEI (GenBank Accession No. AB071286.1) and SBEII (GenBank Accession No. AB194723.1) were downregulated. The WT plant and its modified lines were cultivated in the experimental station, Demonstration Base for Molecular Breeding and New Variety of Sweet Potato (117°15'16", 36°5'56") in Tai'an City (Shandong, China) in early May 2014. The storage roots were harvested in the mid of October 2014, and the starches were isolated using an earlier

method.[25] The obtained starches were dried in an oven at 40 °C for 1 day and were ground and stored in a low-humidity cabinet HZD-1000 (Biofuture Ltd., Beijing, China) for further analyses. As measured using an iodine colorimetric method [7, 26], the apparent amylose content for WT and Waxy-91 was (30.4±0.6)% and (6.7±1.0)%, respectively, while HAM-75, HAM-214, and HAM-234 had apparent amylose contents of (50.3±2.5)%, (65.5±0.6)%, and (61.0±2.6)%, respectively (shown in **Table 1**). The WT and waxy sweet potato starches showed an A-type crystalline structure, and the high-amylose ones presented B-type structures (see XRD patterns in **Fig. S1** in **Supplementary Material**).

Small-angle X-ray Scattering (SAXS). SAXS measurements were conducted on a NanoSTAR system (Bruker, Germany) operated at 30 W. The Cu Kα radiation[27] having a 0.1542 nm wavelength (λ) was used as the X-ray source. Before the SAXS tests, the starch slurries with a starch concentration of *ca.* 40% were kept under ambient conditions for 4 h to achieve equilibrium samples. According to previous research,[28-29] dry starch is in the glassy nematic state, whereas the hydrated starch forms a lamellar smectic structure with highly mobile backbone and spacers. Each starch slurry was placed into the sample cell, which was then exposed at the incident X-ray monochromatic beam for 15 min. The scattering data were collected using a VÅnTeC-2000 detector (active area 140 × 140 mm^2 and pixel size 68 × 68 μm^2). The scattering of an empty cell with water was used as the background data. All data were background subtracted and normalized. The data in the region of *ca.* $0.007 < q < 0.20$ $Å^{-1}$ were used as the SAXS results. The scattering vector, q ($Å^{-1}$), was defined as $q = 4\pi\sin\theta/\lambda$ (2θ, the scattering angle).[30]

Fitting and Analysis of SAXS data. A fitting approach with two Gaussian plus Lorentz peak functions and a power-law function was established to fit the SAXS patterns. The SAXS data were fitted iteratively in Origin 8 software (OriginLab. Inc., USA). The fitting coefficients for each

iteration were refined to minimize the value of chi-squared via a nonlinear, least-squares refinement method. Then, the structural features of starch semicrystalline lamellae were calculated using the linear correlation function (presented in **Eq.(5)**).[31-33]

Size-exclusion Chromatography (SEC). The SEC experiments were conducted according to an earlier method with modifications.[34] The starch was dissolved in a DMSO/LiBr solution containing 0.5% (w/w) LiBr. The possibly-existing non-starch polysaccharides such as cellulose in the sample are mostly insoluble, and were removed by centrifuging the starch-DMSO solution at 4000 *g* for 10 min. The supernatant was mixed with ethanol (6 volumes of DMSO/LiBr) to precipitate the starch, and the precipitated starch was collected by centrifugation at 4000 *g* for 10 min. The precipitated starch was dissolved in DMSO/LiBr at 80 °C overnight. The starch concentration in DMSO/LiBr was determined using the Megazyme total starch assay kit and adjusted to 2 mg/mL for SEC analysis. Briefly, the starch solution was centrifuged at 4000 *g* for 10 min; 2 mL of the supernatant was digested and the glucose released from starch was determined by absorbance at a wavelength of 510 nm using the procedures given by the assay kit manufacturer. To obtain the chain length distributions (CLDs) of debranched starch molecules, the starch samples were debranched using isoamylase according to a previous method.[35] The Agilent 1100 Series SEC system was used, with GRAM precolumn, GRAM 100 and GRAM 1000 columns (PSS, Germany) at a flow rate of 0.6 mL/min. For the debranched starch containing linear molecules, the value of hydrodynamic volume V_h was converted to the degree of polymerization (*DP*) using the Mark–Houwink equation.[36]

Starch Biosynthetic Enzyme Activities Fitted from Number CLDs. A mathematical model was used to fit the number CLDs of debranched amylopectin to parameterize the relative activities of three core classes of starch biosynthetic enzymes, namely, SSs including GBSS, SBE and

148 DBE.[37-38] A theoretical "enzyme set" is defined as a groups of these three enzymes, which includes
149 one of SS, SBE, and DBE, regardless of the actual informs.[37-38] In the present work, the
150 amylopectin CLDs were mainly contributed by enzyme-sets (i) and (ii).

151 **Statistical Analysis.** Data were expressed as means ± standard deviations (SD) and were
152 statistically analyzed using IBM SPSS software version 20.0 (Chicago, IL, USA). A statistical
153 difference of $P < 0.05$ was considered to be significant.

154 **Results and Discussion**

155 **General Features of SAXS Data.** The logarithmic SAXS patterns of WT and modified sweet
156 potato starches are presented in **Fig. S2**. The starches displayed a typical scattering peak at *ca*.
157 0.065 $Å^{-1}$ (labelled as Peak I), ascribed to the widely-reported semicrystalline lamellae in starch.[39]
158 Interestingly, the high-amylose starches, resulting from the downregulated SBE activity, had a less
159 resolved shoulder peak at *ca.* 0.040 $Å^{-1}$ (labelled as Peak II). Such dual-peak scattering pattern of
160 starch semicrystalline lamellae was different from the extensively found results where a single
161 lamellar peak was shown [33, 39]. The results here confirmed the existence of a notable proportion of
162 thicker semicrystalline lamellae (proposed as Type II shown by Peak II) in the high-amylose
163 starches, other than the typical Type I semicrystalline lamellae revealed by the Peak I at *ca*.
164 0.065 $Å^{-1}$.

165 Research has shown the SAXS data of high-amylose maize starches, which have a typical single
166 lamellar peak.[10, 40] Also, the SAXS data for high-amylose potato starches at q values higher than
167 0.02 $Å^{-1}$ were collected.[19] It seems that the used q range could not sufficiently cover the lamellar
168 peak especially at the low angles, and thus it is difficult to observe the full information of lamellar
169 scattering possibly including a dual-peak pattern. In that case, the paracrystalline model
170 accompanied by stacking disorder was applied to describe the lamellar structure, followed by

complicated predefined assumptions of the lamellar stacking and the usage of partial constant lamellar parameters before data fitting.[19] Here, the scattering data in the range of *ca*. $0.007 < q < 0.20$ Å^{-1} were recorded for the sweet potato starches to show the full dual-peak pattern associated with the lamellar structure of the amylose-rich starches. In the following, a fitting method based on combined functions (*e.g*., Gaussian, Lorentz, and power law) was established to fit the net lamellar scattering from the SAXS data. Then, the fitted lamellar scattering was used to acquire the linear correlation function profile with the elimination of non-lamellar scattering.[41] In this way, the fine parameters of the two sub-lamellar fractions (Type I and Type II) with increased accuracy could be calculated straightforwardly.

Fitting of SAXS Data. Two Gaussian plus Lorentz peak functions and a power-law function (Eq. (1)-(3)) were used to fit the scattering data for the high-amylose sweet potato starches with unresolved Peak I and Peak II. This dual-peak fitting method was also applied for the waxy starch (with downregulated GBSSI activity) that did not show a prominent Peak II (**Fig. S2** in **Supplementary Material**), since using only one Gaussian plus Lorentz peak function could not sufficiently fit the scattering pattern (see the single-peak fitting for waxy starch in **Fig. S3** in **Supplementary Material**). Nevertheless, for the WT starch, one Gaussian plus Lorentz peak function (with a power-law function) was enough for the desired fitting.

$$I(q) = B + C * q^{-\delta} + f_1 * G_1(q) + (1 - f_1) * L_1(q) + f_2 * G_2(q) + (1 - f_2) * L_2(q) \quad (1)$$

$$G_x(q) = \frac{A_x\sqrt{\ln 4}}{W_x\sqrt{\frac{\pi}{2}}} \exp\left(-\frac{2\ln 4(q - q_x)^2}{{W_x}^2}\right) \quad (2)$$

$$L_x(q) = \frac{2A_x}{\pi} * \frac{2W_x}{4(q - q_x)^2 + {W_x}^2} \quad (3)$$

In Eq. (1), the first term, B, is the scattering background; the second term, the power-law function in which C and δ are the power-law prefactor and the power-law component, respectively; the third or fifth term, the Gaussian function; the fourth or sixth term, the Lorentz function; f_1 and f_2, the prefactors for Peak I at *ca*. 0.065 Å^{-1} and Peak II at *ca*. 0.040 Å^{-1}, respectively. Again, in Eq. (2) (Gaussian function, $G_x(q)$) and Eq. (3) (Lorentz function, $L_x(q)$), A_x is the peak area, W_x (Å^{-1}) the peak full width at half-maximum (*FWHM*) in reciprocal space, and q_x (Å^{-1}) the peak center position; x = 1 and x = 2 correspond to Peak I and Peak II, respectively. **Fig. 1** shows the SAXS patterns and their fit curves for WT and modified sweet potato starches. The results show that all SAXS patterns could be properly fitted using the above established fitting approach with Eqs. (1)-(3).

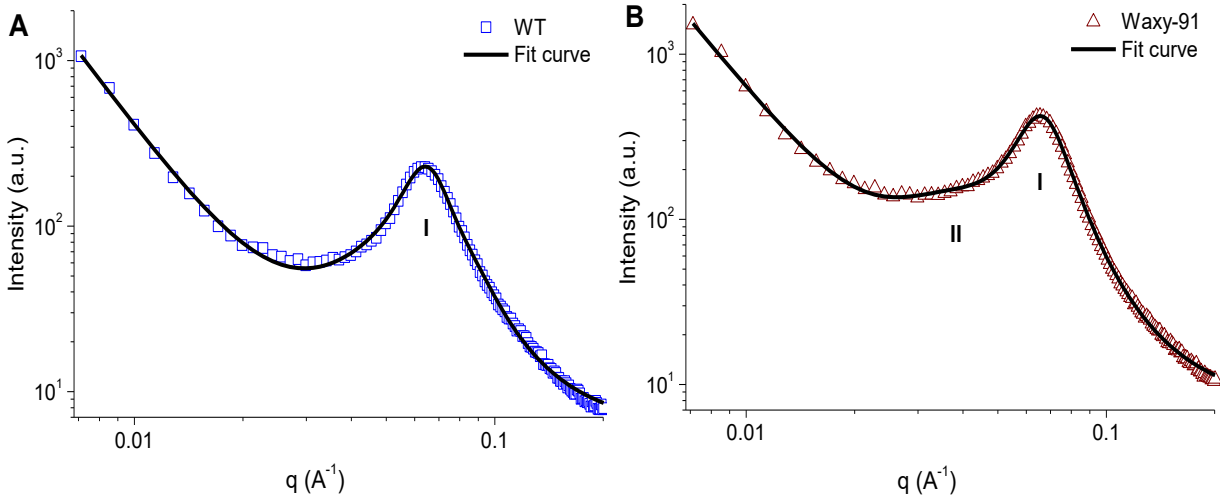

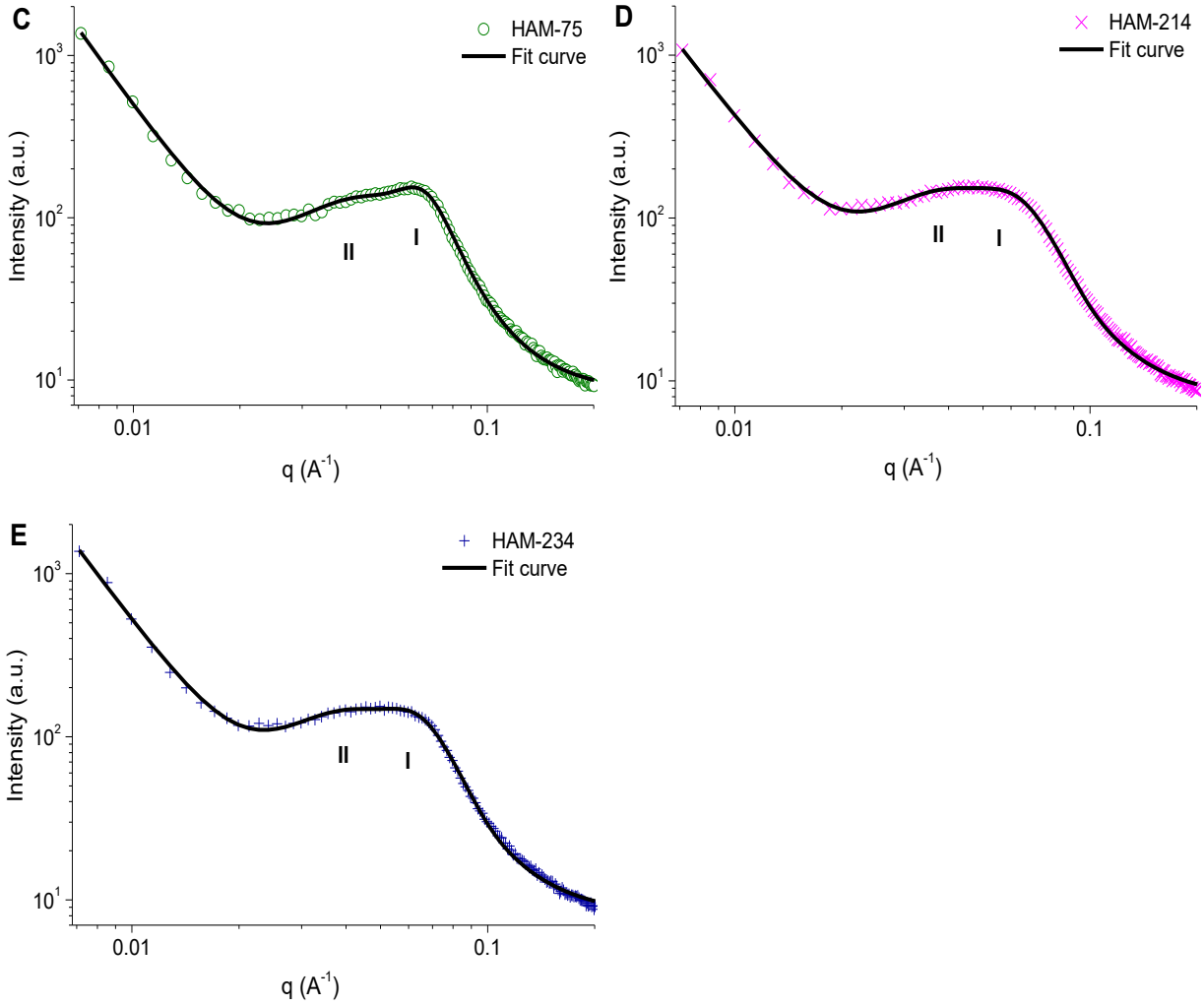

Fig. 1 Logarithmic SAXS patterns and their fit curves of wild-type (WT) (A) and modified (Waxy-91, HAM-75, HAM-214 and HAM-234) (B-E) sweet potato starches.

Thickness Distribution of Semicrystalline Lamellae. By subtracting the background scattering (1st term in Eq. (1)) and the power-law scattering (2nd term in Eq. (1)) from the whole SAXS pattern, the net scattering of lamellar peak could be acquired. Then, the ordinate scattering intensity was normalized using its maximum, and the abscissa q values were transformed into lamellar thickness values equal to $2\pi/q$. Consequently, the thickness distribution profiles of semicrystalline lamellae were revealed for sweet potato starches (**Fig. 2**). The WT starch contained

only Type I semicrystalline lamellae with a single-peak thickness distribution mainly in the range of predominantly 5–20 nm. Nonetheless, the waxy and high-amylose starches displayed a dual-peak lamellar thickness distribution, as they had additional Type II semicrystalline lamellae with a thickness distribution range of mainly 10–50 nm. Note that the waxy sample showed a very weak Type II distribution. That is, compared to GBSSI downregulation, the downregulated SBE activity more effectively induced the formation of Type II semicrystalline lamellae in addition to typical Type I lamellae. This is associated with the altered arrangement of biosynthesized starch molecule chains within the lamellar regions, as discussed especially in the last section.

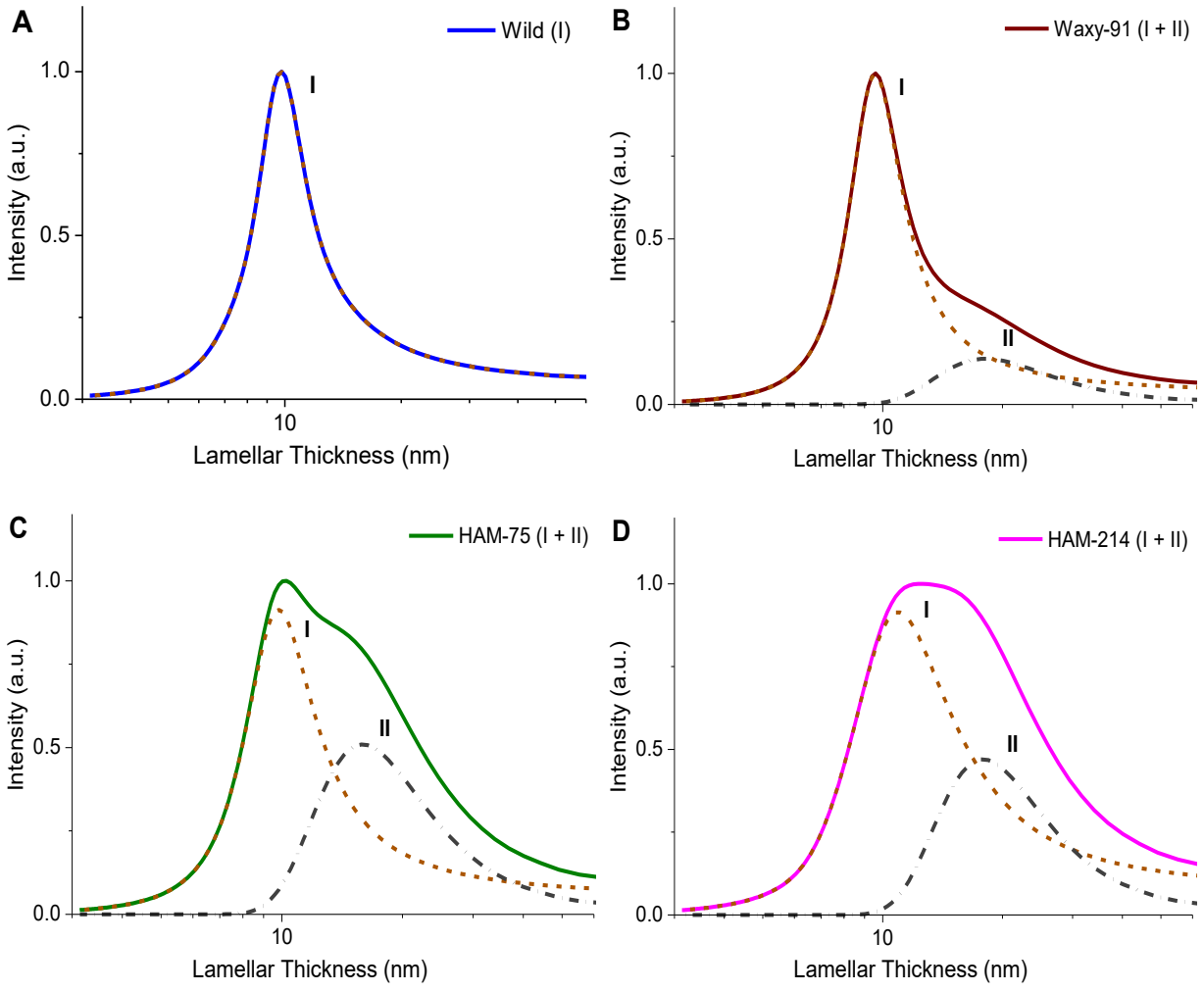

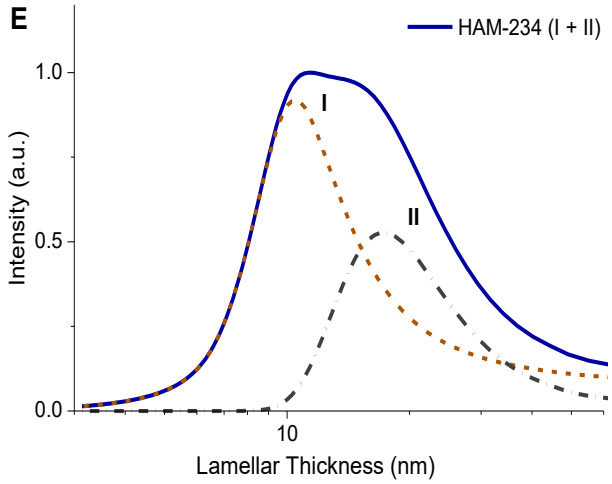

Fig. 2 Semicrystalline lamellar thickness distributions of wild-type (WT) (A) and modified (Waxy-91, HAM-75, HAM-214 and HAM-234) (B-E) sweet potato starches. Solid lines represent whole distribution profiles; short dash lines represent profiles related to Type I semicrystalline lamellae; dash-dot lines represent profiles related to Type II semicrystalline lamellae.

Table 1 shows the fitted peak positions (q_1 and q_2) and *FWHM* values in reciprocal space (W_1 and W_2) for the subpeaks I and II. Then, *FWHM* in reciprocal space was converted into the real space value with Eq. (4). This real space value is positive to the thickness distribution width of semicrystalline lamellae.[42]

$$FWHM(\text{real}) = \frac{2\pi W_x}{{q_x}^2} \quad (4)$$

Here, W_x (Å^{-1}) is the *FWHM* in reciprocal space, and q_x (Å^{-1}) the peak position; subscript x = 1 and x = 2 belong to Peak I and Peak II, respectively. In **Table 1**, Type II lamellae had a larger *FWHM* value than did Type I lamellae. Enhancing SBE downregulation (shown by increased apparent amylose content) led to a gradual increase in *FWHM* for Type I lamellae of all the starches, and a modest increase in this parameter for Type II lamellae of the high-amylose samples.

241 Relative to the amylose-rich starches, the waxy starch had a slightly-increased *FWHM* of Type II
242 lamellae.
243
244 **Table 1** Apparent amylose content and SAXS parameters of wild-type (WT) and modified (Waxy-
245 91, HAM-75, HAM-214 and HAM-234) sweet potato starches [A]

		WT	Waxy-91	HAM-75	HAM-214	HAM-234
	AC	30.4±0.6^{d}	6.7±1.0^{e}	50.3±2.5^{c}	65.5±0.6^{a}	61.0±2.6^{b}
	δ	2.92±0.02^{bc}	2.67±0.03^{d}	3.09±0.03^{a}	2.88±0.03^{c}	2.96±0.03^{b}
Peak I	A_1	4.05±0.12^{b}	8.33±0.14^{a}	3.43±0.50^{c}	4.58±1.11^{bc}	4.15±0.88^{bc}
	q_1 (Å^{-1})	0.0642±0.0001^{b}	0.0656±0.0002^{a}	0.0640±0.0013^{bc}	0.0575±0.0036^{d}	0.0600±0.0028^{cd}
	W_1 (Å^{-1})	0.0256±0.0005^{c}	0.0259±0.0004^{c}	0.0330±0.0019^{b}	0.0417±0.0042^{a}	0.0391±0.0036^{a}
	$FWHM_1$ (nm)	3.90±0.07^{d}	3.77±0.05^{e}	5.05±0.08^{c}	7.92±0.19^{a}	6.82±0.03^{b}
Peak II	A_2	-	1.59±0.18^{b}	2.29±0.46^{a}	1.80±0.96^{ab}	2.04±0.77^{ab}
	q_2 (Å^{-1})	-	0.0347±0.0009^{b}	0.0395±0.0018^{a}	0.0352±0.0023^{b}	0.0364±0.0022^{ab}
	W_2 (Å^{-1})	-	0.0263±0.0027^{a}	0.0294±0.0034^{a}	0.0255±0.0049^{a}	0.0265±0.0042^{a}
	$FWHM_2$ (nm)	-	13.70±0.74^{a}	11.79±0.30^{b}	12.92±0.86^{ab}	12.52±0.50^{ab}
	Chi^2	26.68	58.39	39.81	32.78	42.81

246 [A] *AC*, apparent amylose content (%). Parameters from SAXS data fitting: δ, power-law exponent;
247 A_1 or A_2, lamellar peak area; q_1 or q_2, lamellar peak position; W_1 or W_2, peak full width at half
248 maximum in reciprocal space; $FWHM_1$ or $FWHM_2$, peak full width at half maximum in real space;
249 Chi^2, reduced Chi-square of fitting.

250 [B] The different inline letters within a row indicate significant difference $P < 0.05$.

251

252 **Average Thicknesses of Semicrystalline, Amorphous and Crystalline Lamellae.** The fitted
253 net lamellar peak and its two subpeaks from the whole SAXS pattern were used to calculate the

254 parameters of starch semicrystalline lamellae with increased accuracy.[41] This was achieved using
255 the linear correlation function $f(r)$ in Eq. (5) and **Fig. S4** in **Supplementary Material**.[31-32]

$$f(r) = \frac{\int_0^\infty I(q)q^2 \cos(qr)\,\mathrm{d}q}{\int_0^\infty I(q)q^2\mathrm{d}q} \quad (5)$$

256

257 In Eq. (5), r (nm) is the distance in real space. In **Fig. S4** in **Supplementary Material**, d is the
258 second maximum of $f(r)$ (equal to the average thickness of semicrystalline lamellae); d_a, the
259 average thickness of amorphous lamellae, is acquired by the solution of the linear region and the
260 flat $f(r)$ minimum; d_c, the average thickness of crystalline lamellae, is calculated by $d_c = d - d_a$.

261 **Fig. 3** includes the whole linear correlation function profiles and their subprofiles related to Type
262 I or Type II semicrystalline lamellae for WT and modified sweet potato starches. The second
263 maximum abscissa value (d) of the Type II profile (dash-dot line) was larger than that of the Type
264 I profile (short dash line). Consequently, this abscissa value of the whole profile (real line), related
265 to both Type I and Type II lamellae, ranged somewhere between those two values for the Type I
266 profile and the Type II profile, respectively. Also, relative to the high-amylose starches, the waxy
267 starch had a small Peak II, and thus showed a whole profile close to the Type I profile (**Fig. 3B**).

268

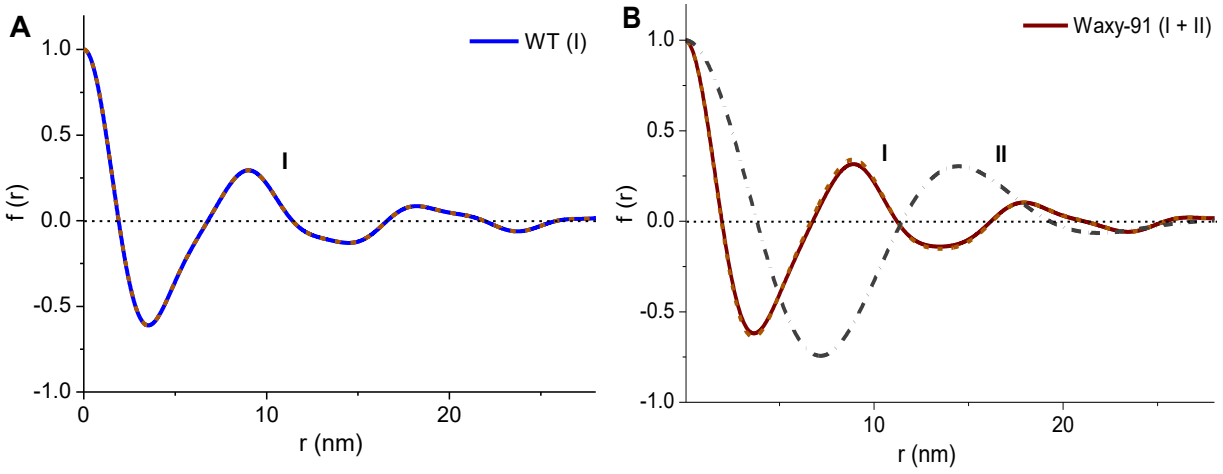

269

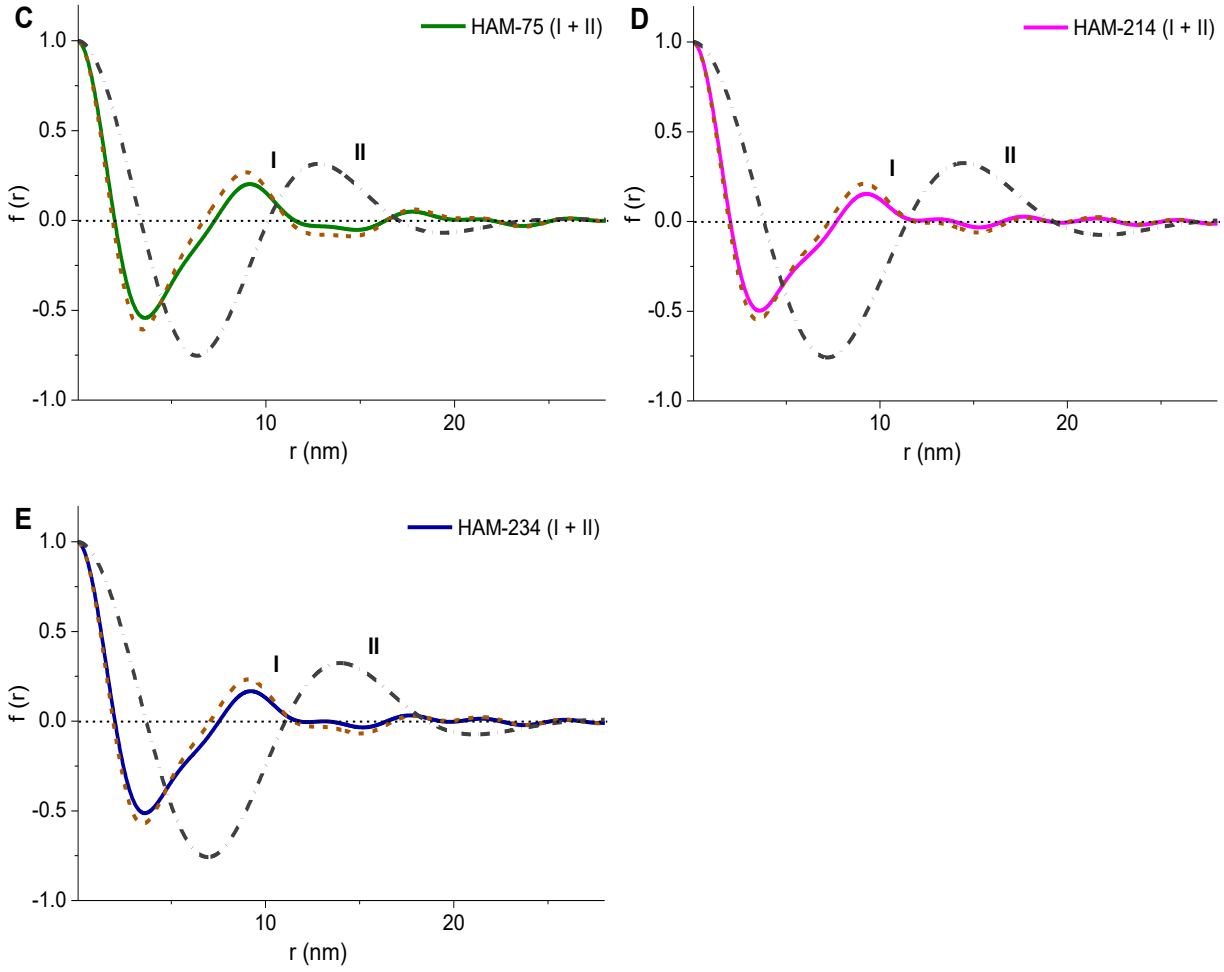

Fig. 3 Linear correlation function profiles of wild-type (WT) (A) and modified (Waxy-91, HAM-75, HAM-214 and HAM-234) (B-E) sweet potato starches. The solid line represents the whole profile; the short dash line represents the profile related to Type I semicrystalline lamellae; the dash-dot line represents the profile related to Type II semicrystalline lamellae.

Table 2 records the lamellar parameters for WT and modified sweet potato starches. Relative to Type I lamellae, Type II lamellae showed thicker amorphous (d_a) and crystalline (d_c) parts, and thus an elevated average thickness (d). For Type I lamellae in high-amylose starches, d_c showed the same trend as d with negligibly changed d_a. This suggests that the downregulated SBE activity

could increase the average thickness of Type I lamellae by thickening the crystalline components rather than the amorphous lamellae. However, Type I lamellae in the waxy sample (with reduced GBSSI expression) had a slight decrease in d_c and an increase in d_a, showing a slightly reduced d relative to that for the WT starch. For Type II lamellae, d_c and d_a showed a constant trend to d, suggesting that the reduced GBSSI or SBE activity tended to simultaneously change the average thicknesses of amorphous and crystalline components with aligned starch molecule chains and thus the overall average thickness.

Table 2 Lamellar parameters of wild-type (WT) and modified (Waxy-91, HAM-75, HAM-214 and HAM-234) sweet potato starches [A]

		WT	Waxy-91	HAM-75	HAM-214	HAM-234
Lamellae I	d_1 (nm)	9.01±0.03^{cB}	8.89±0.04^{d}	8.93±0.03^{d}	9.17±0.04^{a}	9.08±0.03^{b}
	$d_{c\text{-}1}$ (nm)	6.27±0.02^{c}	6.08±0.02^{e}	6.23±0.00^{d}	6.47±0.01^{a}	6.37±0.01^{b}
	$d_{a\text{-}1}$ (nm)	2.74±0.01^{b}	2.81±0.02^{a}	2.70±0.03^{b}	2.70±0.03^{b}	2.71±0.02^{b}
Lamellae II	d_2 (nm)	-	14.47±0.06^{a}	12.78±0.04^{c}	14.48±0.07^{a}	13.96±0.04^{b}
	$d_{c\text{-}2}$ (nm)	-	8.72±0.02^{a}	7.66±0.03^{c}	8.69±0.02^{a}	8.38±0.03^{b}
	$d_{a\text{-}2}$ (nm)	-	5.75±0.04^{a}	5.12±0.01^{c}	5.79±0.05^{a}	5.58±0.01^{b}

[A] Parameters from linear correlation function: d_1 or d_2, the average thickness of Type I or Type II semicrystalline lamellae; $d_{c\text{-}1}$ or $d_{c\text{-}2}$, the average thickness of the crystalline parts of Type I or Type II lamellae; $d_{a\text{-}1}$ or $d_{a\text{-}2}$, the average thickness of the amorphous parts of Type I or Type II lamellae.

[B] The different inline letters within a row indicate significant difference $P < 0.05$.

Chain Length Distributions (CLDs) of Debranched Starch Molecules. To better understand the evolutions of starch chain features as affected by GBSSI or SBE downregulation, we detected the CLDs of debranched WT and modified sweet potato starches expressed as weight distribution

300 $w_{de}(\log DP)$ (**Fig. 4**). Despite that SEC results might suffer from inaccuracies related to band
301 broadening and the calibration between *DP* and elution volume [43], this issue is insignificant for the
302 present work for semi-quantitative purposes [44]. In **Fig. 4**, the WT starch showed typical weight
303 CLDs with amylopectin chains of $DP < 100$ and amylose chains of $DP \geq 100$. There were two
304 peaks existing in the range of amylopectin chains. The first peak represents the short amylopectin
305 chains with *DP* up to 32, and the second peak comprises the long amylopectin chains with *DP* 33–
306 100. When the GBSSI activity was reduced, the resultant waxy starch displayed largely reduced
307 amylose chains (decreased apparent amylose content) but relatively increased long amylopectin
308 chains. In contrast, the SBE downregulation for high-amylose samples allowed three main kinds
309 of alteration to CLDs: (1) The first peak for short amylopectin chains centered at a higher *DP* but
310 still covered *DP* up to 32; (2) The second peak for long amylopectin chains also moved to a higher
311 *DP* and located in a largely-broadened range of *DP* 33–200; (3) The first and second peaks showed
312 a reduction and an increase in height respectively, suggesting the relatively reduced amounts of
313 short amylopectin chains or increased amounts of long amylopectin chains. These phenomena
314 became more evident when we enhanced the suppression of SBE as indicated by the increased
315 apparent amylose content. Moreover, the trend of apparent amylose content of HAM-75 < HAM-
316 234 < HAM-214 shown in the section on materials could be confirmed by the changes in the
317 relative area under the CLD curve for amylose chains.
318

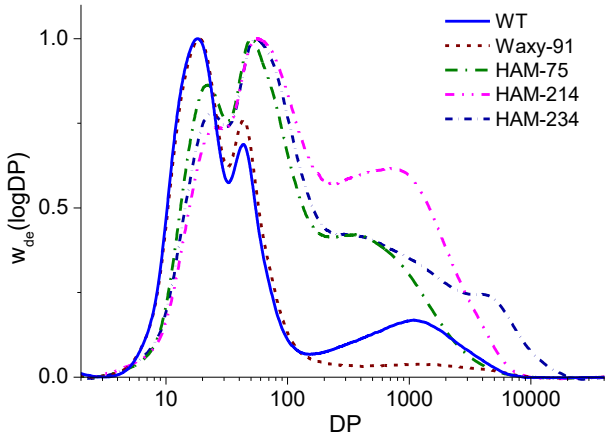

Fig. 4 SEC weight distributions of debranched wild-type (WT) and modified (Waxy-91, HAM-75, HAM-214 and HAM-234) sweet potato starches.

Parameterized Biosynthetic Enzyme Activities for Starch. The weight distributions for WT and waxy sweet potato starches were converted into the number distribution $N_{de}(DP)$ following $w_{de}(DP) = DP^2 N_{de}(DP)$,[36] and the number CLDs for amylopectin chains with $DP < 100$ are plotted in **Fig. 5**. A modelling method was applied to fitting the number CLDs to provide information on the relative activities of the core starch biosynthetic enzymes such as SS, SBE and DBE.[38] As confirmed in **Fig. 5**, the amylopectin chains were predominantly synthesized by two enzyme-sets, namely, the enzyme-set (i) fitted from $DP \leq 32$ chains (orange fit curve) and the enzyme-set (ii) fitted from *DP* 33 to 60–70 chains (pink fit curve).

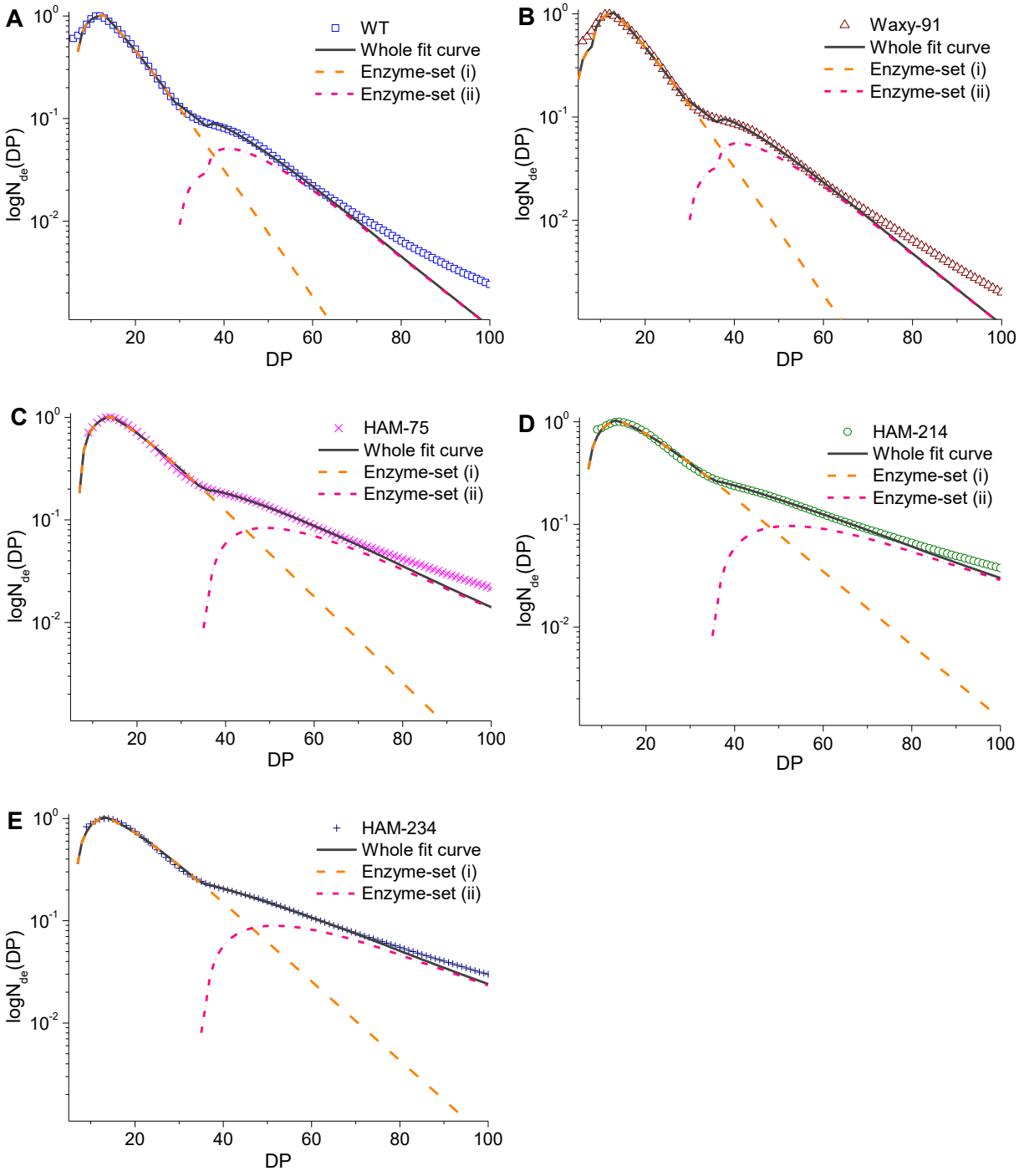

Fig. 5 Number chain length distributions and their fit curves of debranched wild-type (WT) (A) and modified (Waxy-91, HAM-75, HAM-214 and HAM-234) (B-E) sweet potato starches. The black solid line represents the whole fit curve for chains from enzyme-sets (i) and (ii); The orange

dash line represents the fit curve for chains from enzyme-set (i); the pink dash-dot line represents the fit curve for chains from enzyme-set (ii).

Six parameters were acquired from the fitting, including $\beta_{(i)}$ and $\beta_{(ii)}$ representing the relative activity of SBE to SS within the corresponding enzyme-set, $\gamma_{(i)}$ and $\gamma_{(ii)}$ denoting the relative activity of DBE to SS within each enzyme-set, and $h_{(i)}$ and $h_{(ii)}$ indicating the relative contribution of each enzyme-set to the whole CLDs. **Table 3** lists the fitted enzyme activity parameters. No prominent differences could be seen for the six parameters among WT and waxy sweet potato starches, reflecting that reducing GBSSI expression correlated with amylose synthesis did not significantly affect the activity ratios of SBE:SS and DBE:SS as well as the contributions of enzyme-sets to the amylopectin CLDs. However, compared to the WT starch, the values of $\beta_{(i)}$, $\beta_{(ii)}$, $\gamma_{(i)}$, and $\gamma_{(ii)}$ reduced significantly for the high-amylose starches, followed by substantially increased $h_{(ii)}$ but negligibly changed $h_{(i)}$. This indicates that reducing SBE activity caused not only an expectable reduction in the activity ratio of SBE:SS but also a decrease in the activity ratio of DBE:SS, with a relatively elevated contribution of chains from enzyme-set (ii) to the whole CLDs. Again, like for the CLD evolutions in the section on CLD results, these changes were more prominent with reduced SBE activity as indicated by the increased amylose level.

Table 3 Parameterized biosynthetic enzyme parameters of wild-type (WT) and modified (Waxy-91, HAM-75, HAM-214 and HAM-234) sweet potato starches [A]

	WT	Waxy-91	HAM-75	HAM-214	HAM-234
$\beta_{(i)}$	0.1035±0.0016^{aB}	0.1047±0.0012^{a}	0.0688±0.0005^{b}	0.0598±0.0021^{d}	0.0639±0.0016^{c}
$\beta_{(ii)}$	0.0553±0.0006^{a}	0.0558±0.0003^{a}	0.0333±0.0002^{b}	0.0271±0.0003^{d}	0.0288±0.0007^{c}

$\gamma_{(i)}$	0.0599±0.0004 [a]	0.0604±0.0003 [a]	0.0470±0.0002 [b]	0.0445±0.0010 [c]	0.0463±0.0007 [b]
$\gamma_{(ii)}$	0.0451±0.0004 [a]	0.0450±0.0005 [a]	0.0321±0.0002 [b]	0.0256±0.0003 [d]	0.0275±0.0008 [c]
$h_{(i)}$	1.0158±0.0103 [ab]	1.0239±0.0066 [a]	1.0137±0.0025 [b]	1.0269±0.0011 [a]	1.0292±0.0038 [a]
$h_{(ii)}$	0.0539±0.0039 [b]	0.0585±0.0039 [b]	0.0833±0.0005 [a]	0.0906±0.0082 [a]	0.0859±0.0049 [a]

[A] $\beta_{(i)}$ or $\beta_{(ii)}$, activity ratio of SBE:SS from enzyme-set (i) or (ii); $\gamma_{(i)}$ or $\gamma_{(ii)}$, activity ratio of DBE:SS from enzyme-set (i) or (ii); $h_{(i)}$ or $h_{(ii)}$, relative contribution of enzyme-set (i) or (ii) to the whole chain length distributions.

[B] The different inline letters within a row indicate significant difference $P < 0.05$.

Discussion on How GBSSI or SBE Downregulation Alters Starch Lamellae. With the CLD results and the fitted enzyme parameters, a schematic representation was proposed for the lamellar structure of starch following GBSSI or SBE downregulation (**Fig. 6**). The biosynthesis of starch chains and their subsequent alignment in lamellae involve the actions of different biosynthetic enzymes.[45-46] Particularly, the glucan chains form by transferring the glucosyl units of ADP-glucose to non-reducing ends of pre-existing glucans via new α-(1,4)-linkages through soluble SSs mainly for amylopectin and GBSS (GBSSI in storage tissues and GBSSII in other tissues) primarily for amylose.[45, 47] SBEs create new glucan branches by catalyzing the cleavage of α-(1,4)-linkages and transfer of the released reducing ends to glucose residues on the original or another glucan chains via α-(1,6)-linkages.[48-49] DBEs such as the isoamylases trim the improperly positioned branches preventing local crystallization or side chain clustering.[50-51] Here, for the WT starch from a regular cultivar, the enzyme-set (i) primarily but not exclusively synthesized the short amylopectin chains ($DP \leq 32$) confined in single crystalline lamellae to construct the well-known lamellar structure (Type I semicrystalline lamellae in the WT starch in **Fig. 6A**), and some of the long amylopectin branches ($33 \leq DP < 60$–70) protruding the single lamella space to enter the contiguous amorphous lamellae (even the subsequent crystalline lamellae) [38]. The other long

379 amylopectin chains were predominantly from the enzyme-set (ii), and protruded the single
380 crystalline lamellae to remain in the contiguous, amorphous lamellae.[37-38, 44]
381

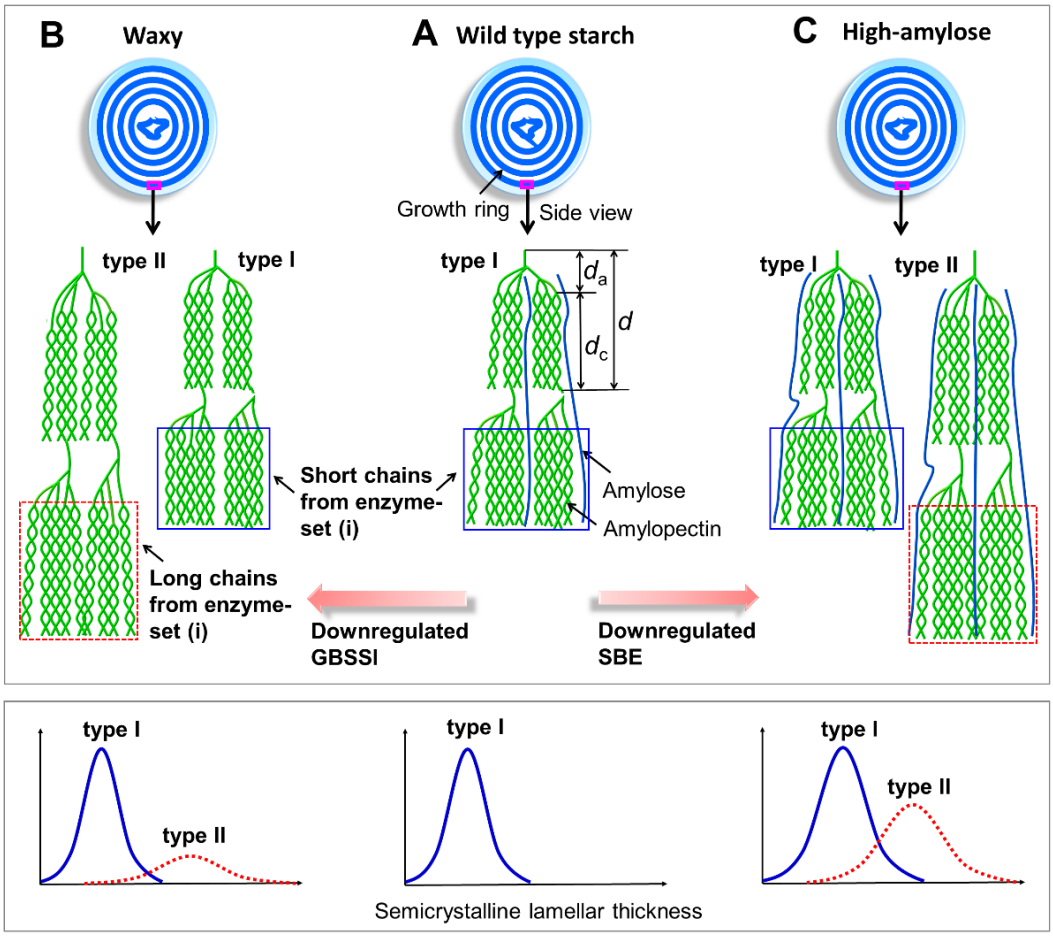

382

383 **Fig. 6** Schematic representation of the lamellar structure of sweet potato starch following GBSSI
384 or SBE downregulation. GBSSI, granule-bound starch synthase I; SBE, starch branching enzyme.
385

386 For the waxy starch, the reduced activity of GBSSI could slow the synthesis of amylose
387 accordingly, contributing to providing relatively more glucose substrate for soluble SSs to elongate
388 amylopectin branches. SSI elongates the shortest amylopectin chains with *DP* 6–7 to form *DP* ~9–
389 12 chains.[52] SSII elongates the chains from SSI to generate *DP* < 30 chains and the subsequent

products are further elongated by SSIII to create long chains (*DP* higher than 30).[53-54] There are two isoforms for SSII and SSIII, including SSIIa and SSIIIa in storage tissues and SSIIb and SSIIIb in leave tissues.[45] Thus, it can be deduced that SSIII specifically SSIIIa in tuber had a relatively stronger contribution to the synthesis of amylopectin chains, generating an increased proportion of long chains with *DP* 33–100 (shown in **Fig. 4**). Though the formation of long amylopectin chains might be also related to the reduced SBE activity,[55] the constant activity ratios of SBE:SS and DBE:SS (discussed in the section on biosynthesis enzyme activities) could make this scenario insignificant. Regarding the lamellar stacking, it can be proposed that part of the long amylopectin chains ($DP \geq 33$) from enzyme-set (i), actually the so-called single-lamella set,[38] could be confined to the single crystalline lamellae of Type II lamellar structure like the manner of short chains ($DP \leq 32$) from enzyme-set (i) to typical Type I lamellae (illustrated in **Fig. 6B**). Agreeing on this, the increased lamellar thicknesses such as d_c of Type II lamellae (see the section on lamellar thicknesses) confirmed the need for longer chains packed in Type II single crystalline lamellae. Again, the rest of long chains from enzyme-set (i) and the long chains from enzyme-set (ii) could still span more than a single-lamella range like the counterpart chains located in the WT starch. Hence, this is the first work revealing that the amylopectin chains from enzyme-set (i) might be classified as three subfractions rather than two subgroups reported previously [38], namely, the short chains confined to single crystalline lamellae of Type I lamellar structure, the long chains arranged to thicker single crystalline lamellae of Type II structure, and the long chains protruding single crystalline lamellae.

For the high-amylose starches, the reduced activity ratios of SBE:SS and DBE:SS (the section on biosynthesis enzyme activities) altered the chain features and thus the chain assembly in the lamellar structure. Specifically, SBE has two types, involving SBEI and SBEII preferentially

transferring the glucan chains of different lengths. SBEI is apt to branch long chains such as amylose and transfer longer branches; SBEII tends to branch highly-branched amylopectin and transfer short branches.[49] The reduced SBEII expression, with the SSs still elongating amylopectin chains, certainly hindered the generation of short amylopectin chains (reflected by the shift of the short chain peak to higher *DP* values in **Fig. 4** in the section on CLD results) but significantly enhanced the formation of long amylopectin chains (confirmed by the stronger peak for long chains in **Fig. 4**). The lowered activity of SBEI and the steady action of GBSS to elongate amylose chains could allow the synthesis of increased amylose chains probably with higher *DP* values (shown in **Fig. 4**). In addition, the lowered SBE activity with normal SSs including GBSS reduced the possibility for the generation of improperly positioned chains, weakening the need of DBEs to trim these chains (see reduced DBE:SS activity ratio in the section on biosynthesis enzyme activities). Analogous to the lamellae in the waxy starch, Type I lamellae were mainly constructed by $DP \leq 32$ short chains from the single-lamella enzyme-set (i); the right-shifted peak of these short chains (suggesting an increased average chain length) resulted in the emergence of thickened crystalline lamellae (an increased d_c) constructing the semicrystalline lamellae with a larger d. Type II crystalline lamellae contained part of long amylopectin chains with *DP* above 33 to form the related lamellar structure with an increase average thickness (**Fig. 6C**). Again, the enhancement of SBE downregulation could enhance the evolutions in chain features and thus in the lamellar structural parameters.

To conclude, the downregulated GBSSI or SBE activity could give rise to the formation of additional semicrystalline lamellae (named Type II) in sweet potato starch, other than the typical lamellae (Type I) found previously. A fitting approach based on two Gaussian plus Lorentz peak functions with a power-law function was established to successfully resolve the net lamellar peak

436 and its two subpeaks related to Type I and Type II lamellar structures respectively from the whole
437 SAXS pattern; then, the fine features of the two kinds of amorphous-crystalline lamellae were
438 disclosed with the linear correlation function. Relative to Type I lamellae, Type II lamellae showed
439 increases in the average thickness (*d*) and the thickness distribution width (*FWHM*), followed by
440 simultaneously thickened amorphous (d_a) and crystalline (d_c) parts. These lamellar structural
441 features could be further regulated by simply controlling the enzyme type (*e.g.*, GBSSI and SBE)
442 for activity downregulation and the activity downregulation degree for a specific enzyme such as
443 SBE.

444 Then, the chain length distributions in sweet potato starches and the relative activities of
445 biosynthetic enzymes were analyzed to help understand how the reduced GBSSI or SBE activity
446 influences the starch lamellar structure. Note that mainly two starch biosynthetic enzyme-sets,
447 namely, enzyme-set (i) and enzyme-set (ii), were confirmed to synthesize the glucan chains of
448 amylopectin. Along with the actions of other biosynthetic enzymes, the decreased GBSSI or SBE
449 activity tended to relatively increase the amount of amylopectin long chains with a degree of
450 polymerization (DP) $\geq$ 33. Part of these long chains from the single-lamella enzyme-set (i) could
451 be confined to the single crystalline lamella space of Type II lamellar structure, whereas the short
452 chains of $DP \leq 32$ could be aligned within the crystalline parts of Type I lamellae, with the rest
453 long chains from enzyme-set (i) and the long chains from enzyme-set (ii) located in more than a
454 single lamella. Hence, this work enables an in-depth understanding of the new lamellar structural
455 features in sweet potato starch as induced by GBSSI or SBE downregulation, which is valuable
456 for the rational production of similar starch resources with regulated structure and thus
457 performance for different food products.

458 ASSOCIATED CONTENT

Supporting Information (SI) is available free of charge on the ACS Publications website at DOI: xxx. See SI for supplementary Tables and Figure.

AUTHOR INFORMATION

Corresponding Author

* Peng Zhang. Email: zhangpeng@sibs.ac.cn

† Fengwei Xie. Email: f.xie@uq.edu.au, fwhsieh@gmail.com

Author Contributions

The manuscript was written through contributions of all authors. All authors have given approval to the final version of the manuscript.

Notes

The authors declare no competing financial interest.

ACKNOWLEDGMENT

The authors would like to acknowledge the National Natural Science Foundation of China (NSFC) (Project Nos. 31701637 and 31801582), the Fundamental Research Funds for the Central Universities (Project No. 2662016QD008), the Chinese Academy of Sciences (Project No. XDPB04), and the Project funded by China Postdoctoral Science Foundation (Project No. 2018M642865). B. Zhang thanks the Young Elite Scientists Sponsorship Program by China Association for Science and Technology, the Chutian Sholars Program of Hubei Province, and the Shishan Sholars Program of Huazhong Agricultural University. F. Xie acknowledges the support of the European Union's Marie Skłodowska-Curie Actions (MSCA) and the Institute of Advanced

Study (IAS), University of Warwick for the Warwick Interdisciplinary Research Leadership Programme (WIRL-COFUND). The authors also thank Dr. Cheng Li, Dr. Enpeng Li and Mr. Shiqing Zhou from Prof. Robert G. Gilbert's lab at Yangzhou University for their assistance on SEC analysis.

ABBREVIATIONS

GBSSI, Granule-bound starch synthase I; SBE, starch branching enzyme; DP, degree of polymerization; AGPase, ADP-glucose pyrophosphorylase; SSs, starch synthases; SBEs, starch branching enzymes; DBEs, starch debranching enzymes; WT, wild-type; SAXS, small-angle X-ray scattering; CLDs, chain length distributions; FWHM, peak full width at half-maximum.

REFERENCES

1. Lee, Y.; Choi, M.-S.; Lee, G.; Jang, S.; Yoon, M.-R.; Kim, B.; Piao, R.; Woo, M.-O.; Chin, J. H.; Koh, H.-J., Sugary Endosperm is Modulated by Starch Branching Enzyme IIa in Rice (Oryza sativa L.). *Rice* **2017,** *10* (1), 33.

2. Wang, Y.; Li, Y.; Zhang, H.; Zhai, H.; Liu, Q.; He, S., A soluble starch synthase I gene, IbSSI, alters the content, composition, granule size and structure of starch in transgenic sweet potato. *Sci. Rep.* **2017,** *7* (1), 2315-2315.

3. Zobel, H. F., Molecules to Granules: A Comprehensive Starch Review. *Starch - Stärke* **1988,** *40* (2), 44-50.

4. French, D., Fine Structure of Starch and its Relationship to the Organization of Starch Granules. *Journal of the Japanese Society of Starch Science* **1972,** *19* (1), 8-25.

5. Tester, R. F.; Karkalas, J.; Qi, X., Starch—composition, fine structure and architecture. *J. Cereal Sci.* **2004,** *39* (2), 151-165.

6. Donald, A. M.; Waigh, T. A.; Jenkins, P. J.; Gidley, M. J.; Debet, M.; Smith, A., Internal structure of starch granules revealed by scattering studies. In *Starch: Structure and Functionality*, Frazier, P. J.;

503 Donald, A. M.; Richmond, P., Eds. The Royal Society of Chemistry: Cambridge, 1997; pp 172-179.
504 7. Zhou, W.; Yang, J.; Hong, Y.; Liu, G.; Zheng, J.; Gu, Z.; Zhang, P., Impact of amylose content on
505 starch physicochemical properties in transgenic sweet potato. *Carbohydr. Polym.* **2015,** *122*, 417-427.
506 8. Jobling, S., Improving starch for food and industrial applications. *Curr. Opin. Plant Biol.* **2004,** *7*
507 (2), 210-218.
508 9. Qiao, D.; Yu, L.; Liu, H.; Zou, W.; Xie, F.; Simon, G.; Petinakis, E.; Shen, Z.; Chen, L., Insights
509 into the hierarchical structure and digestion rate of alkali-modulated starches with different amylose
510 contents. *Carbohydr. Polym.* **2016,** *144*, 271-281.
511 10. Blazek, J.; Gilbert, E. P., Effect of Enzymatic Hydrolysis on Native Starch Granule Structure.
512 *Biomacromolecules* **2010,** *11* (12), 3275-3289.
513 11. Liu, H. S.; Xie, F. W.; Yu, L.; Chen, L.; Li, L., Thermal processing of starch-based polymers. *Prog.*
514 *Polym. Sci.* **2009,** *34* (12), 1348-1368.
515 12. Xie, F.; Halley, P. J.; Avérous, L., Rheology to understand and optimize processibility, structures
516 and properties of starch polymeric materials. *Prog. Polym. Sci.* **2012,** *37* (4), 595-623.
517 13. Cameron, R. E.; Donald, A. M., A Small-Angle X-Ray-Scattering Study of the Absorption of Water
518 into the Starch Granule. *Carbohydr. Res.* **1993,** *244* (2), 225-236.
519 14. Cameron, R. E.; Donald, A. M., A Small-Angle X-Ray-Scattering Study of Starch Gelatinization
520 in Excess and Limiting Water. *Journal of Polymer Science Part B-Polymer Physics* **1993,** *31* (9), 1197-
521 1203.
522 15. Daniels, D. R.; Donald, A. M., Soft material characterization of the lamellar properties of starch:
523 Smectic side-chain liquid-crystalline polymeric approach. *Macromolecules* **2004,** *37* (4), 1312-1318.
524 16. Zhang, B.; Chen, L.; Li, X.; Li, L.; Zhang, H., Understanding the multi-scale structure and
525 functional properties of starch modulated by glow-plasma: A structure-functionality relationship. *Food*
526 *Hydrocolloid* **2015,** *50*, 228-236.
527 17. Qiao, D.; Tu, W.; Zhang, B.; Wang, R.; Li, N.; Nishinari, K.; Riffat, S.; Jiang, F., Understanding
528 the multi-scale structure and digestion rate of water chestnut starch. *Food Hydrocolloid* **2019,** *91*, 311-318.

18. Hernández-Hernández, E.; Ávila-Orta, C. A.; Hsiao, B. S.; Castro-Rosas, J.; Gallegos-Infante, J. A.; Morales-Castro, J.; Araceli Ochoa-Martínez, L.; Gómez-Aldapa, C. A., Synchrotron X-ray scattering analysis of the interaction between corn starch and an exogenous lipid during hydrothermal treatment. *J. Cereal Sci.* **2011,** *54* (1), 69-75.

19. Gomand, S. V.; Lamberts, L.; Gommes, C. J.; Visser, R. G.; Delcour, J. A.; Goderis, B., Molecular and morphological aspects of annealing-induced stabilization of starch crystallites. *Biomacromolecules* **2012,** *13* (5), 1361-70.

20. Bie, P.; Li, X.; Xie, F.; Chen, L.; Zhang, B.; Li, L., Supramolecular structure and thermal behavior of cassava starch treated by oxygen and helium glow-plasmas. *Innov. Food Sci. Emerg.* **2016,** *34*, 336-343.

21. Blazek, J.; Gilbert, E. P., Application of small-angle X-ray and neutron scattering techniques to the characterisation of starch structure: A review. *Carbohydr. Polym.* **2011,** *85* (2), 281-293.

22. Koroteeva, D. A.; Kiseleva, V. I.; Krivandin, A. V.; Shatalova, O. V.; Blaszczak, W.; Bertoft, E.; Piyachomkwan, K.; Yuryev, V. P., Structural and thermodynamic properties of rice starches with different genetic background Part 2. Defectiveness of different supramolecular structures in starch granules. *Int J Biol Macromol* **2007,** *41* (5), 534-47.

23. Koroteeva, D. A.; Kiseleva, V. I.; Sriroth, K.; Piyachomkwan, K.; Bertoft, E.; Yuryev, P. V.; Yuryev, V. P., Structural and thermodynamic properties of rice starches with different genetic background: Part 1. Differentiation of amylopectin and amylose defects. *Int J Biol Macromol* **2007,** *41* (4), 391-403.

24. Yang, J.; Bi, H.-P.; Fan, W.-J.; Zhang, M.; Wang, H.-X.; Zhang, P., Efficient embryogenic suspension culturing and rapid transformation of a range of elite genotypes of sweet potato (Ipomoea batatas [L.] Lam.). *Plant Sci.* **2011,** *181* (6), 701-711.

25. Zhao, S.; Dufour, D.; Sánchez, T.; Ceballos, H.; Zhang, P., Development of waxy cassava with different Biological and physico-chemical characteristics of starches for industrial applications. *Biotechnol. Bioeng.* **2011,** *108* (8), 1925-1935.

26. Tan, I.; Flanagan, B. M.; Halley, P. J.; Whittaker, A. K.; Gidley, M. J., A method for estimating the nature and relative proportions of amorphous, single, and double-helical components in starch granules

555 by C-13 CP/MAS NMR. *Biomacromolecules* **2007,** *8* (3), 885-891.

556 27. Zhang, B.; Bai, B.; Pan, Y.; Li, X. M.; Cheng, J. S.; Chen, H. Q., Effects of pectin with different
557 molecular weight on gelatinization behavior, textural properties, retrogradation and in vitro digestibility of
558 corn starch. *Food Chem.* **2018,** *264*, 58-63.

559 28. Waigh, T. A.; Perry, P.; Riekel, C.; Gidley, M. J.; Donald, A. M., Chiral side-chain liquid-
560 crystalline polymeric properties of starch. *Macromolecules* **1998,** *31* (22), 7980-7984.

561 29. Waigh, T. A.; Kato, K. L.; Donald, A. M.; Gidley, M. J.; Clarke, C. J.; Riekel, C., Side-chain liquid-
562 crystalline model for starch. *Starch/Stärke* **2000,** *52* (12), 450-460.

563 30. Suzuki, T.; Chiba, A.; Yano, T., Interpretation of small angle X-ray scattering from starch on the
564 basis of fractals. *Carbohydr. Polym.* **1997,** *34* (4), 357-363.

565 31. Goderis, B.; Reynaers, H.; Koch, M. H. J.; Mathot, V. B. F., Use of SAXS and linear correlation
566 functions for the determination of the crystallinity and morphology of semi-crystalline polymers.
567 Application to linear polyethylene. *Journal of Polymer Science Part B-Polymer Physics* **1999,** *37* (14),
568 1715-1738.

569 32. Wang, C.; Liao, W. P.; Cheng, Y. W., Strong diffuse scattering and lamellar morphologies of
570 syndiotactic polystyrene: Polymorphic effects. *Journal of Polymer Science Part B-Polymer Physics* **2003,**
571 *41* (20), 2457-2469.

572 33. Qiao, D.; Xie, F.; Zhang, B.; Zou, W.; Zhao, S.; Niu, M.; Lv, R.; Cheng, Q.; Jiang, F.; Zhu, J., A
573 further understanding of the multi-scale supramolecular structure and digestion rate of waxy starch. *Food*
574 *Hydrocolloids* **2017,** *65*, 24-34.

575 34. Shi, L. F.; Fu, X.; Tan, C. P.; Huang, Q.; Zhang, B., Encapsulation of Ethylene Gas into Granular
576 Cold-Water-Soluble Starch: Structure and Release Kinetics. *J. Agric. Food Chem.* **2017,** *65* (10), 2189-
577 2197.

578 35. Hasjim, J.; Lavau, G. C.; Gidley, M. J.; Gilbert, R. G., In Vivo and In Vitro Starch Digestion: Are
579 Current in Vitro Techniques Adequate? *Biomacromolecules* **2010,** *11* (12), 3600-3608.

580 36. Liu, W.-C.; Halley, P. J.; Gilbert, R. G., Mechanism of Degradation of Starch, a Highly Branched

581 Polymer, during Extrusion. *Macromolecules* **2010,** *43* (6), 2855-2864.
582 37. Wu, A. C.; Gilbert, R. G., Molecular Weight Distributions of Starch Branches Reveal Genetic
583 Constraints on Biosynthesis. *Biomacromolecules* **2010,** *11* (12), 3539-3547.
584 38. Wu, A. C.; Morell, M. K.; Gilbert, R. G., A Parameterized Model of Amylopectin Synthesis
585 Provides Key Insights into the Synthesis of Granular Starch. *PLoS ONE* **2013,** *8* (6).
586 39. Zhang, B.; Xie, F.; Shamshina, J. L.; Rogers, R. D.; McNally, T.; Halley, P. J.; Truss, R. W.; Chen,
587 L.; Zhao, S., Dissolution of Starch with Aqueous Ionic Liquid under Ambient Conditions. *ACS Sustainable*
588 *Chemistry & Engineering* **2017,** *5* (5), 3737-3741.
589 40. Shrestha, A. K.; Blazek, J.; Flanagan, B. M.; Dhital, S.; Larroque, O.; Morell, M. K.; Gilbert, E. P.;
590 Gidley, M. J., Molecular, mesoscopic and microscopic structure evolution during amylase digestion of
591 maize starch granules. *Carbohydr. Polym.* **2012,** *90* (1), 23-33.
592 41. Zhang, B.; Xie, F.; Wang, D. K.; Zhao, S.; Niu, M.; Qiao, D.; Xiong, S.; Jiang, F.; Zhu, J.; Yu, L.,
593 An improved approach for evaluating the semicrystalline lamellae of starch granules by synchrotron SAXS.
594 *Carbohydr. Polym.* **2017,** *158*, 29-36.
595 42. Cardoso, M. B.; Westfahl, H., On the lamellar width distributions of starch. *Carbohydr. Polym.*
596 **2010,** *81* (1), 21-28.
597 43. Cave, R. A.; Seabrook, S. A.; Gidley, M. J.; Gilbert, R. G., Characterization of Starch by Size-
598 Exclusion Chromatography: The Limitations Imposed by Shear Scission. *Biomacromolecules* **2009,** *10* (8),
599 2245-2253.
600 44. Wang, K.; Hasjim, J.; Wu, A. C.; Henry, R. J.; Gilbert, R. G., Variation in Amylose Fine Structure
601 of Starches from Different Botanical Sources. *J. Agric. Food Chem.* **2014,** *62* (19), 4443-4453.
602 45. Tetlow, I. J., Starch biosynthesis in developing seeds. *Seed Science Research* **2011,** *21* (1), 5-32.
603 46. Castro, J. V.; Dumas, C.; Chiou, H.; Fitzgerald, M. A.; Gilbert, R. G., Mechanistic information
604 from analysis of molecular weight distributions of starch. *Biomacromolecules* **2005,** *6* (4), 2248-2259.
605 47. Ball, S. G.; Morell, M. K., From bacterial glycogen to starch: Understanding the biogenesis of the
606 plant starch granule. *Annu. Rev. Plant Biol.* **2003,** *54*, 207-233.

607 48. Rahman, S.; Regina, A.; Li, Z. Y.; Mukai, Y.; Yamamoto, M.; Kosar-Hashemi, B.; Abrahams, S.;
608 Morell, M. K., Comparison of starch-branching enzyme genes reveals evolutionary relationships among
609 isoforms. Characterization of a gene for starch-branching enzyme IIa from the wheat D genome donor
610 Aegilops tauschii. *Plant Physiol.* **2001,** *125* (3), 1314-1324.
611 49. Nakamura, Y.; Utsumi, Y.; Sawada, T.; Aihara, S.; Utsumi, C.; Yoshida, M.; Kitamura, S.,
612 Characterization of the Reactions of Starch Branching Enzymes from Rice Endosperm. *Plant Cell Physiol*
613 **2010,** *51* (5), 776-794.
614 50. Delatte, T.; Trevisan, M.; Parker, M. L.; Zeeman, S. C., Arabidopsis mutants Atisa1 and Atisa2
615 have identical phenotypes and lack the same multimeric isoamylase, which influences the branch point
616 distribution of amylopectin during starch synthesis. *Plant J.* **2005,** *41* (6), 815-830.
617 51. Wattebled, F.; Planchot, V.; Dong, Y.; Szydlowski, N.; Pontoire, B.; Devin, A.; Ball, S.; D'Hulst,
618 C., Further Evidence for the Mandatory Nature of Polysaccharide Debranching for the Aggregation of
619 Semicrystalline Starch and for Overlapping Functions of Debranching Enzymes in Arabidopsis Leaves.
620 *Plant Physiol.* **2008,** *148* (3), 1309-1323.
621 52. Fujita, N.; Yoshida, M.; Asakura, N.; Ohdan, T.; Miyao, A.; Hirochika, H.; Nakamura, Y., Function
622 and characterization of starch synthase I using mutants in rice. *Plant Physiol.* **2006,** *140* (3), 1070-1084.
623 53. Umemoto, T.; Yano, M.; Satoh, H.; Shomura, A.; Nakamura, Y., Mapping of a gene responsible
624 for the difference in amylopectin structure between japonica-type and indica-type rice varieties. *Theor Appl*
625 *Genet* **2002,** *104* (1), 1-8.
626 54. Fujita, N.; Yoshida, M.; Kondo, T.; Saito, K.; Utsumi, Y.; Tokunaga, T.; Nishi, A.; Satoh, H.; Park,
627 J.-H.; Jane, J.-L.; Miyao, A.; Hirochika, H.; Nakamura, Y., Characterization of SSIIIa-Deficient mutants of
628 rice: The function of SSIIIa and pleiotropic effects by SSIIIa deficiency in the rice endosperm. *Plant Physiol.*
629 **2007,** *144* (4), 2009-2023.
630 55. Wang, K.; Wambugu, P. W.; Zhang, B.; Wu, A. C.; Henry, R. J.; Gilbert, R. G., The biosynthesis,
631 structure and gelatinization properties of starches from wild and cultivated African rice species (Oryza
632 barthii and Oryza glaberrima). *Carbohydr. Polym.* **2015,** *129*, 92-100.
633

- Table of Contents -

Changes in Nanoscale Chain Assembly in Sweet Potato Starch Lamellae by Downregulation of Biosynthesis Enzymes

Binjia Zhang [a], *Wenzhi Zhou* [b], *Dongling Qiao* [c], *Peng Zhang* [*,b], *Siming Zhao* [a], *Liang Zhang* [d], *Fengwei Xie* [†,e,f]